



## On the relation between the echo-peak shift and Brownian-oscillator correlation function

Wim P. de Boeij, Maxim S. Pshenichnikov, Douwe A. Wiersma

*Ultrafast Laser and Spectroscopy Laboratory, Department of Chemistry, Materials Science Centre, University of Groningen, Nijenborgh 4, 9747 AG Groningen, The Netherlands*

Received 16 January 1996

---

### Abstract

We show that for systems that exhibit bimodal dynamics in their system–bath correlation function the shift of the stimulated photon-echo maximum as a function of waiting time reflects fairly well the long time part of the correlation function. For early times this correspondence breaks down due to a fundamentally different behaviour of the echo-peak shift in this time domain and because of the effect of finite pulse duration on the echo-peak shift. The method is used to characterize the solvation dynamics in various dye solutions.

---

### 1. Introduction

The exploration of solvation dynamics is currently actively pursued using a variety of methods [1,2]. There are at least two good reasons for this activity. First, a grasp of solvation dynamics is crucial to a better understanding of chemical reactivity in the liquid phase. Second, novel theoretical approaches to a description of solvation dynamics have emerged. Especially molecular dynamics simulation studies of solvation dynamics [3–8] and calculations based on an instantaneous modes analysis [9,10] of solvent motion have provided a different perspective and stimulated new experiments. For instance, the so-called inertial solvation effect was first observed in computer simulations [3] and predicted to occur on a 100 fs timescale. Since then this inertial effect has been searched for in many ultrafast (nonlinear) optical experiments.

The most direct probe of solvation dynamics is time-gated fluorescence [11–14]. The achievable time resolution is about 100 fs, and is set by the fact that a careful balance between both spectral and time resolution must be maintained. The analysis of this experiment is, however, not as straightforward as it seems [14]; especially the fitting of the short-time dynamics is problematic. Transient absorption studies [15] have a much higher time-resolution intrinsically, but here interference with stimulated emission presents a problem. Another popular probe of solvation dynamics is femtosecond photon echo [16–27]. This technique has a time resolution limited only by the excitation pulse width, which can be about 10 fs. A clear disadvantage of this method is the fact that a theoretical model is needed to connect the echo with the solvation dynamical process.

The connection between the optical and solvation dynamics is often made through the multi-mode

Brownian oscillator (MBO) model [28]. In certain limits this model reduces to the Kubo stochastic-oscillator model and to the Bloch model. Here the total system is partitioned in a two-level electronic system coupled to a bath comprised of the remaining degrees of freedom. In the MBO model a central role is played by the oscillator-bath correlation function  $M(t)$ , which, in linear response theory, is isomorphous with the solvation-correlation function. Many recent femtosecond photon echo experiments have employed the MBO model to elucidate  $M(t)$  [19,20,22–27]. The problem is that the correlation function  $M(t)$  is not directly expressed in the measured photon echo response. Even in the impulsive excitation limit, calculation of the time-gated echo signal involves a double time-integration of  $M(t)$  [23,26]. When the time-integrated echo is measured by a slow detector an additional time integration is required. It is therefore highly desirable to develop a simple method that yields a first-order approximation to the correlation function.

In this paper we discuss echo-maximum (-peak) shift measurements and show that under certain conditions the echo-peak shift reflects fairly well the correlation function. An echo-peak shift experiment is based on a conventional time-integrated stimulated photon echo (SPE) experiment, with delay  $\tau$  between the first two excitation pulses and  $T$  between the second and third pulses. The observable is the shift of the position of the echo maximum on scanning  $\tau$  at a certain fixed  $T$ . This shift is then measured as a function of  $T$  (waiting time).

Echo-peak shift measurements were first explored by the Ippen group in three-pulse scattering studies on condensed phase systems [29,30]. It was clearly demonstrated that the echo-peak shift is related to the balance between homogeneous and inhomogeneous broadening in the system. Joo and Albrecht employed echo-peak shift measurements to characterize spectral diffusion in optical transitions of dyes in solution, using a stochastic model to interpret the data [21]. Recently Joo et al. sought to employ the echo-peak shift as probe of the inertial effect in solvation dynamics [25]. We questioned their analysis and pointed out that for early times the photon echo-peak shift is dominated by wave packet dynamics and finite excitation pulsewidth effects rather than solvation dynamics [27]. Subsequently, in nu-

merical simulations of SPE we found that the echo-peak shift is directly related to the correlation function<sup>1</sup>.

In this Letter we show that an essential prerequisite for a correspondence between the echo-peak shift and the correlation function is the presence of an initial fast component in the system-bath correlation function. The similarity breaks down, however, at short timescales due to fundamentally different behaviour of the echo-peak shift and due to finite pulse-width effects on the echo shift. Computer simulations and results of echo-peak shift measurements in different solvents are reported and briefly discussed.

## 2. Theoretical background

In this section we investigate the relation between the echo-peak shift and the correlation function  $M(t)$  in the context of the MBO model. The MBO model has been described extensively in the literature [28] so we will mention only a few points relevant to this Letter. In the MBO model all intra-, intermolecular and solvent motions are represented by harmonic oscillators that can be over- or underdamped. For example, a molecular vibration is portrayed by an underdamped oscillator, and solvent motions are simulated by a set of different overdamped Brownian oscillators. An important ingredient in the MBO model is the so-called line broadening function  $g(t)$ . Once  $g(t)$  is known, all nonlinear optical response functions can be calculated, including the ones that determine the shift of the echo maximum. The line shape function  $g(t)$  is connected to the correlation function  $M(t)$  in the following way:

$$g(t) = i\lambda \int_0^t d\tau [M(\tau) - 1] + \Delta^2 \int_0^t d\tau_1 \int_0^{\tau_1} d\tau_2 M(\tau_2) \quad (1)$$

<sup>1</sup> The remarkable similarity between the echo-peak shift and correlation function was first discussed at the VII-th Time-Resolved Vibrational Spectroscopy Meeting (Ref. [31]).

In Eq. (1),  $\lambda$  equals half the distance between the first momenta of the absorption and emission spectra, while  $\Delta$  is connected to the frequency and displacement of the Brownian oscillator. In the high temperature limit the parameters  $\Delta$  and  $\lambda$ , are related by  $\Delta^2 \approx 2\lambda kT/\hbar$ . The extension to a multi-mode model is straightforward;  $g(t)$  is just the sum over single-oscillator functions,  $g_i(t)$ :  $g(t) = \sum_i g_i(t)$ .

In conventional SPE experiments the echo signal is measured using a slow detector, thereby recording the integrated transient. It has been shown that the SPE intensity can be expressed in terms of  $g(t)$  as follows [20]

$$I_{\text{SPE}}(T, \tau) \propto \exp(-2T/T_1) \int_0^\infty dt \cos^2[\text{Im}\{g(t) + g(T) - g(t+T)\}] \times \exp[-2 \text{Re}\{g(t) + g(\tau) - g(T) + g(t+T) + g(\tau+T) - g(\tau+t+T)\}] \quad (2)$$

In Eq. (2)  $t$  is the time of the echo with respect to the third pulse, while  $T_1$  denotes the population relaxation time. For a general  $M(t)$  it is not feasible to calculate the echo-shift analytically from Eq. (2). Yet it turns out that an analytical solution is possible when  $M(t)$  exhibits bimodal dynamics, with a dominant fast initial part  $M_{\text{fast}}(t)$  and a slower tail  $M_{\text{slow}}(t)$ :

$$M(t) = (1-a)M_{\text{fast}} + aM_{\text{slow}} \quad \text{with } a \ll 1 \quad (3)$$

Interestingly enough a correlation function of this form is often applicable to optical dynamics in solution. The fast part of  $M(t)$  could be due to multi-wavepacket dynamics [30] or/and the inertial solvation effect [3–8].

In the theoretical analysis following it is assumed that  $M_{\text{fast}}(T)$  has decayed to zero at time  $T$ :  $M_{\text{fast}}(T) = 0$ . The slow part of the correlation function is taken to be stationary on the timescales of  $t$  and  $\tau$ . With these assumptions we can expand  $g(T+t)$  in a Taylor series around  $g(T)$ . The resulting expressions for the real and imaginary parts are then found to be:

$$\text{Im}\{g(T+t)\} \approx \text{Im}\{g(T)\} - i\lambda t[1 - aM_{\text{slow}}(T)]$$

$$\text{Re}\{g(T+t)\} \approx \text{Re}\{g(T)\} + \Delta^2 t \int_0^T M(\tau) d\tau + \frac{\Delta^2 t^2}{2} aM_{\text{slow}}(T) \quad (4)$$

The time-integrated echo signal can be calculated by substitution of the above expressions into Eq. (2) as:

$$I(T, \tau) \propto \exp(-2T/T_1) \int_0^\infty dt \cos^2\{\text{Im}\{g(t)\} + \lambda t[1 - aM_{\text{slow}}(T)]\} \times \exp\{-2 \text{Re}\{g(t) + g(\tau)\} + 2\Delta^2 \tau t aM_{\text{slow}}(T)\} \quad (5)$$

To obtain the shift of the echo maximum as a function of  $\tau$ , the derivative of  $I(T, \tau)$  with respect to  $\tau$  must be taken and the zero-crossing point be found:

$$\left. \frac{dI(T, \tau)}{d\tau} \right|_{\tau=S(T)} = 0 \quad (6)$$

Here  $S(T)$  denotes the measured echo-maximum shift as a function of the waiting time  $T$ . Applying Eq. (6) to Eq. (5), results in the following transcendental equation for  $S(T)$ :

$$S(T) \sqrt{\pi} (\beta^2 - \Delta^2) \{1 + \text{erf}[\beta S(T)]\} + \beta \exp[-\beta^2 S^2(T)] = 0, \quad (7)$$

where

$$\beta = \frac{aM_{\text{slow}}(T) \Delta^2}{\sqrt{\Delta^2 + \lambda^2 [1 - aM_{\text{slow}}(T)]}} \quad (8)$$

and  $\text{erf}(x)$  is the error function. Solving Eqs. (7) and (8) and using the fact that  $a \ll 1$ , the following relation between the correlation function and the echo shift is found:

$$M_{\text{slow}}(T) \approx \frac{\sqrt{\pi} (\Delta^2 + \lambda^2)}{a} S(T) \quad (9)$$

Eq. (9) is the main result of this paper. It shows that a direct one-to-one relationship exists between the echo-shift and the ‘‘slow’’ part of the correlation function. We hasten to stress that a crucial factor to obtaining the result of Eq. (9) is that the correlation function exhibits bimodal dynamics as expressed by

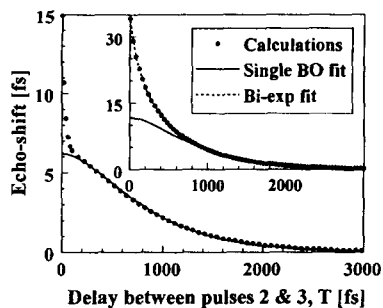


Fig. 1. Calculated echo-peak shift functions for scenarios where the fastest part of the correlation function is included (main figure) and neglected (inset). The fit parameters are given in Table 1. The total coupling strength  $\Delta$  was set at  $265 \text{ cm}^{-1}$  (50 THz). The solid circles represent results of numerical simulations while the solid lines are fits as described in the text.

Eq. (3). Note also that the echo-shift provides information on the correlation function regardless of population relaxation, as is the case in conventional SPE (Eq. (2)).

Fig. 1 vividly demonstrates the remarkable correspondence that can exist between the echo-peak shift and the slow part of the correlation function. For simplicity, the calculations were performed for  $\delta$ -pulse excitation conditions. For the case to be discussed the correlation function was taken as the sum of two critically damped Brownian oscillators [28]:

$$M(t) = A_f \exp(-\omega_f t) [1 + \omega_f t] + A_s \exp(-\omega_s t) [1 + \omega_s t] \quad (10)$$

The chosen oscillator parameters are listed in Table 1. To judge on the measure of correspondence, the Ansatz is that the echo-peak shift function (calculated from the true correlation function Eq. (10)) has the same time dependence as the slow part of the correlation function itself, with  $\omega$ , and  $A_s$  being fit parameters. As can be seen in Fig. 1, the fit calcu-

lated on the basis of this assumption accords very well with the echo shifts calculated from the input correlation function. The similarity of the two sets of data starts already from early waiting times ( $\approx 100$  fs), with fit parameters that are within 20% of those used for the input correlation function (Table 1). On the other hand, if only the slow Brownian oscillator is taken as  $M(t)$ , the calculated echo-peak shift fails completely to represent the correlation function (Fig. 1, inset). Nonetheless, even in this case the long times echo shift (from 1 ps on) provides a good approximation of the correlation function (Table 1). This latter case is a clear demonstration of the fact that an appreciable initial relaxation is required to have the echo-peak shift reflect the correlation function. For example, a double-exponential fit, shown as the dashed line in the inset of Fig. 1, yields decays of 110 fs (32%) and 600 fs (68%). Although the 600 fs decay time correctly reflects the tail of the correlation function, the fast decay time has no physical significance.

We will now show that there is a fundamental reason why the echo-maximum-shift cannot represent the correlation function at early times. This fact is related to the theoretical requisite that the slope of the correlation function near zero time should vanish [3]. For the echo-peak-shift function this slope will be shown to be distinctly non-zero. To quantify the above statement, we first expand the system's correlation function at early times to second order:

$$M(t) \approx 1 - \frac{\omega^2 t^2}{2} \quad (11)$$

Using Eqs. (1), (2), (6) and (11) it can then be shown that the following relation exists between the

Table 1  
Parameters of the fits presented in Fig. 1. Amplitudes of the oscillators are normalized so  $\sum_i A_i = 1$

Parameter	Fig. 1		Fig. 1, inset	
	Input for $M(t)$	Fit on $S(T)$ <sup>a</sup>	Input for $M(T)$	Fit on $S(T)$ <sup>b</sup>
$A_s$	0.5	0.41	1	1
$(\omega_s)^{-1}$ (fs)	500	450	500	475
$A_f$	0.5	–	0	–
$(\omega_f)^{-1}$ (fs)	50	–	–	–
$A_0$ (fs)	–	15	–	12

<sup>a</sup> Fit was performed from  $T = 100$  fs on.

<sup>b</sup> Fit was performed from  $T = 1$  ps on.

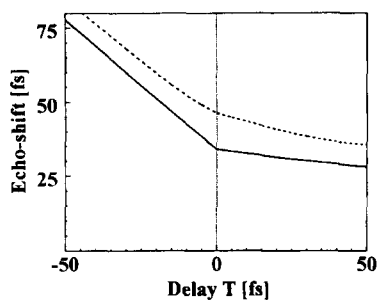


Fig. 2. The initial behaviour of the echo-peak shift. Solid and dotted lines are for  $\delta$ -pulses and 15-fs pulses excitation, respectively. The parameters are the same as for the inset of Fig. 1. The detuning of the laser from the absorption maximum was set to zero.

zero-time slope of echo-shift and echo-shift function itself at that time:

$$\left( \frac{\partial S(T)}{\partial T} \right)_{T \rightarrow +0} \approx - \frac{1}{2 + \frac{4}{3} \Delta^2 S^2(T=0) [1 + 2\omega^2 S^2(T=0)]}, \quad (12)$$

From Eq. (12) it follows immediately that the initial slope of the echo-maximum shift function is always negative. To illustrate this point in more detail, the situation near zero delay for the shift of the echo maximum is displayed in Fig. 2. From these simulations we found also that the slope of the

echo-shift function can be described fairly well by Eq. (12).

When a finite pulse width is taken into account the situation remains basically the same. To illustrate this let us first consider the echo-shift behaviour for negative delays  $T$ , where the position of the pulses 2 and 3 is interchanged. In order to generate any three pulse echo signal, the delay between the first two pulses should be small enough for the electronic coherence to survive. This can be only accomplished for delays  $\tau$  that are close to the absolute value of the waiting time  $T$ . This manifests itself as a straight line in the echo-peak-shift plot (Fig. 2), which exhibits a slope of approximately  $-1$ . For finite excitation pulse widths the general trend persists, although the whole shift function is somewhat displaced to larger echo-peak-shift values (Fig. 2, dotted line). Moreover, an additional contribution to the echo-shift around  $T = 0$  can be noticed, which results from the convolution of the echo-peak shift and the excitation pulse width. Therefore, the overall conclusion must be that the echo-shift function is not suitable for the characterization of the short-time decay of the correlation function.

Let us turn now to a more realistic correlation function  $M(t)$  as encountered in experiments on dye solutions and examine its correspondence to the echo-shift function  $S(t)$ . Previous time-gated echo experiments [23] demonstrated that in solution  $M(t)$  is distinctly bimodal, with the fast part caused by wave packet dynamics and, possibly, the inertial effect and the slower part by diffusive solvent mo-

Table 2

Parameters of the fits presented in Fig. 3. The amplitudes of the oscillators are normalized so  $\sum_i A_i = 1$ . The fit was performed from  $T = 40$  fs on

Parameter	Input correlation function $M(t)$	Fit to $S(T)$ for:	
		$\delta$ -pulses	15-fs pulses
$A_1$	0.37	0.41	0.44
$(A_1)^{-1}$ (fs)	140	150	140
$A_2$	0.13	0.16	0.13
$(A_2)^{-1}$ (ps)	5	5.3	3.9
$A_3$	0.26	0.15	0.16
$A_v$	0.24	0.28	0.27
$(\gamma_v)^{-1}$ (fs)	190	170	165
$\omega_v$ ( $\text{cm}^{-1}$ )	154	153	154
$A_0$ (fs)	–	13.0	14.7
$t_0$ (fs)	–	–15	–21

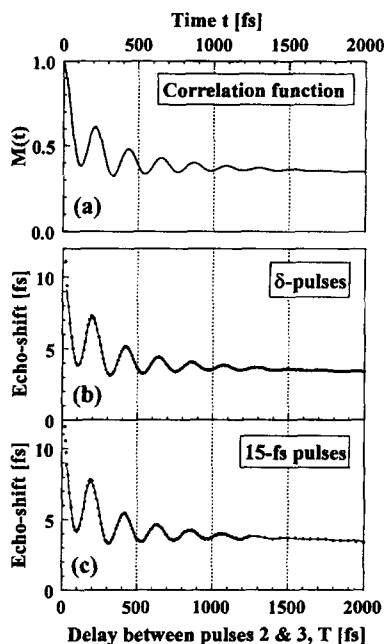


Fig. 3. A model correlation function (a) and calculated echo-peak shift for  $\delta$ -pulses excitation (b) and 15-fs pulses excitation (c). Parameters of the fits are given in Table 2. In numerical simulations of the echo-peak shift, the total coupling strength  $\Delta$  was set at  $300 \text{ cm}^{-1}$  (55 THz) and the detuning of the laser from the absorption maximum was  $450 \text{ cm}^{-1}$  to the red. Note the striking similarity between the correlation function (a) and echo-shift (b, c) regardless of the pulse duration.

tion. To simulate solvent and intramolecular vibrational dynamics we therefore consider a correlation function based on a set of four Brownian oscillators:

$$M(t) = A_1 \exp(-\Lambda_1 t) + A_2 \exp(-\Lambda_2 t) + A_3 + A_v \exp(-\gamma_v t/2) \times \left[ \cos \Omega_v t + \frac{\gamma_v}{(2\Omega_v)} \sin \Omega_v t \right] \quad (13)$$

where  $\Omega_v = [(\omega_v)^2 - (\gamma_v/2)^2]^{1/2}$ . The first three terms represent solvent motion, while the term with amplitude  $A_v$  represents an intramolecular vibrational mode with frequency  $\omega_v$  and decay time  $\gamma_v$ . The Brownian oscillator parameters used are listed in Table 2. Fig. 3 shows that a remarkable similarity exists between the correlation function and the echo-peak shift calculated from the correlation function. To quantify the correspondence, the calculated echo-peak shifts were fitted using the original corre-

lation function, be it that the amplitude  $A_0$  and zero-time-shift  $t_0$  were added as additional fit parameters,  $S(T) = A_0 M(T - t_0)$ . Fit parameters for both impulsive and finite pulse-width excitation are given in Table 2 and show that a reasonable correspondence exists with the input parameters, although the amplitude  $A_1$  of the fastest oscillator is over- and that of the static one  $A_3$  under-estimated. The correspondence for both impulsive and finite pulse-width excitation holds because a 15-fs pulse is short compared to the vibrational period ( $\approx 200 \text{ fs}$ ). A non-zero time shift  $t_0$  appears since we displayed on the abscissa axis the delay between the second and third pulses  $T$  rather than that between the first and third pulses  $t_{13} = T + \tau$ , upon which the vibrational coherence mainly depends [32]. This fact is not captured by Eq. (9) due to the approximations made.

The excellent correspondence between the echo-peak shift and correlation function in the case discussed rests upon the presence of a marked vibrational contribution to the correlation function. At early times ( $t \leq 100 \text{ fs}$ ) this mode leads to a fast decay of  $M(t)$ , which is connected to the short-time dynamics of the underdamped mode. When this mode exhibits its first recurrence, the fastest exponential solvent mode  $A_1$  has taken over the role of the underdamped mode in providing an ultrafast decay of  $M(t)$ . This means that the total correlation function still complies with the condition set by Eq. (3).

In closing this section we note that time-gated SPE is superior to echo-peak shift measurements in characterization of the correlation function, because the integration over time  $t$  in Eqs. (2) and (5) is absent. It can be shown that in this case both the slow and fast part of the correlation function as well as their relative strengths (Eq. (3)) can be determined, without having to make the assumption that  $a \ll 1$  [33].

### 3. Results and discussion

We have applied the method outlined above to the study of solvation dynamics in three different solvents: ethylene glycol (EG), methanol (MeOH) and acetonitrile (AN). As a probe, the dye molecule DTTCl was taken, although some other molecules from the same carbocyanine group (HITCl, HDITCP,

DDTTCI) were also used as probes. The echo-peak-shift experiments were performed as described in Refs. [27] and [29] and will be presented in more detail elsewhere [33]. The echo-peak shift functions obtained looked very similar to those shown in Fig. [3]. In light of the preceding discussion we may therefore assume the echo-shift function to be a fair representation of the correlation function beyond, say,  $T = 50$  fs. Multiple prominent vibrational modes as well as several overdamped modes were evident in the experimental signals. The data were fitted in the form analogous Eq. (13) using seven Brownian oscillators. In order to describe the inertial solvation effect, a Gaussian initial part was also incorporated in the fit. Since the vibrational contributions were identical for all solvents, we concluded that they reflect the intra-molecular modes and are not related to the true solvation dynamics. In sharp contrast, the other (overdamped) modes were found to be strongly solvent dependent and only weakly dependent on the probe molecule. Therefore, we can most likely assign these overdamped modes to solvation dynamics. By eliminating the vibrational effect from the fitted echo-peak shift curves, we are left with the genuine solvation correlation function (Fig. 4). Note, that an ultrafast part of it, which is probed in phase-locked pump-probe experiments [27,34], is not displayed; with the fit starting at 50 fs this part is automatically omitted. The ultrafast part of the correlation function is currently assigned by us to intramolecular energy redistribution after instantaneous (at the timescale of the pulse duration) excitation of a vibrational manifold that underlies the optical spectrum excited.

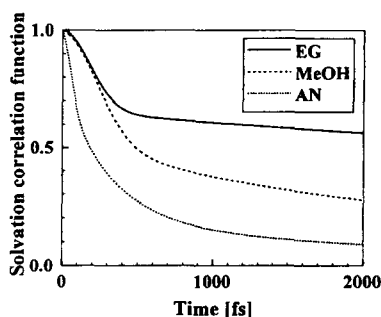


Fig. 4. Initial part of the solvation correlation function for ethylene glycol (EG), methanol (MeOH) and acetonitrile (AN).

The ultrafast part of the depicted correlation functions up to times of 200 fs is very similar for the solvents methanol and ethylene glycol. It is tempting to assign this effect to librational motion of the OH-group. A much faster initial decay of the solvation correlation function is observed for acetonitrile. The long time dynamics is slowest for ethylene glycol (up to 300 ps). In acetonitrile and methanol, the slower solvation steps occur on timescales of 3 and 6 ps, respectively. All these timescales are in good agreement with those reported by Horng et al. [14], although we observed longer decay times for ethylene glycol and acetonitrile. In particular, the  $1/e$  decay times of the correlation function ( $t_{1e}$ ), 0.33 ps (acetonitrile), 1.1 ps (methanol) and 14.5 ps (ethylene glycol) are very similar to those reported by Horng et al. [14]. The results for methanol accord also well with those reported by the Bingemann et al. [15] (although our data show no indication of an initial solvation process on a timescale of 70 fs) and are in line with data presented in Ref. [13]. From phase-locked pump-probe experiments [34] we deduced a dynamical process on a 40 fs timescale, which we have assigned here to an intramolecular vibrational redistribution effect.

#### 4. Summary and conclusion

Conventional stimulated photon echo-maximum shift experiments yield important information on the system–bath correlation function for systems that exhibit ultrafast initial dynamics. Such fast dynamics can be provided by, for instance, the combination of inertial solvation response and wavepacket dynamics. A theoretical analysis of the relation between the echo-shift and system–bath correlation function has been presented in the framework of the Brownian oscillator model. The short-time dynamics is not reflected correctly in the echo-shift due to different behaviour of the echo-shift and correlation function at early times. This implies that echo-maximum shift measurements cannot be used for a final characterization of the correlation function. To get the full picture of the solute–solvent dynamics, time-gated [23,26] and phase-locked heterodyne-detected [27,34,35] stimulated photon echo are the most powerful tools.

## Acknowledgements

We are grateful to Foppe de Haan for providing us with software for efficient data-collection and handling. We also would like to thank Dr. Maxim Mostovoy of the Theoretical Physics Department for helpful suggestions on the mathematics of the problem. The investigations were supported by the Netherlands Foundation for Chemical Research (SON) and Physical Research (FOM) with financial aid from the Netherlands Organization for the Advancement of Science (NWO).

## References

- [1] A.H. Zewail, *Femtochemistry: Ultrafast dynamics of the chemical bond* (World Scientific, Singapore, 1994).
- [2] D.A. Wiersma, ed., *Proceedings of the colloquium femtosecond reaction dynamics* (North-Holland, Amsterdam, 1994) and references therein.
- [3] G. van der Zwan and J.T. Hynes, *J. Phys. Chem.* 89 (1985) 4181.
- [4] M. Maroncelli, *J. Chem. Phys.* 94 (1991) 2084.
- [5] E.A. Carter and J.T. Hynes, *J. Chem. Phys.* 94 (1991) 5961.
- [6] L. Perera and M.L. Berkowitz, *J. Chem. Phys.* 96 (1992) 3092; *ibid.* 97 (1992) 5253.
- [7] E. Neria and A. Nitzan, *J. Chem. Phys.* 96 (1992) 5433.
- [8] M. Maroncelli, V.P. Kumar and A. Papazyan, *J. Phys. Chem.* 97 (1993) 13.
- [9] B.M. Ladanyi and R.M. Stratt, *J. Phys. Chem.* 99 (1995) 2502.
- [10] R.M. Stratt and M. Cho, *J. Chem. Phys.* 100 (1994) 6700.
- [11] S.J. Rosenthal, X. Xie, M. Du and G.R. Fleming, *J. Chem. Phys.* 95 (1991) 4715.
- [12] R. Jimenez, G.R. Fleming, P.V. Kumar and M. Maroncelli, *Nature* 369 (1994) 471.
- [13] T. Gustavsson, G. Baldacchino, J.-C. Mialocq and S. Pommeret, *Chem. Phys. Letters* 236 (1995) 587.
- [14] M.L. Horng, J. Gardecki, A. Papazyan and M. Maroncelli, *J. Phys. Chem.* 99 (1995) 17311.
- [15] D. Bingemann and N.P. Ernstring, *J. Chem. Phys.* 102 (1995) 2691.
- [16] P.C. Becker, H.L. Fragnito, J.Y. Bigot, C.H. Brito Cruz, R.L. Fork and C.V. Shank, *Phys. Rev. Letters* 63 (1989) 505.
- [17] J.Y. Bigot, M.T. Portella, R.W. Schoenlein, C.J. Bardeen, A. Migus and C.V. Shank, *Phys. Rev. Letters* 66 (1991) 1138.
- [18] E.T.J. Nibbering, D.A. Wiersma and K. Duppen, *Phys. Rev. Letters* 66 (1991) 2464.
- [19] E.T.J. Nibbering, K. Duppen and D.A. Wiersma, *J. Photochem. Photobiol. A: Chem.* 62 (1992) 347.
- [20] E.T.J. Nibbering, Ph.D. Thesis, Groningen, The Netherlands (1993).
- [21] T. Joo and A.C. Albrecht, *Chem. Phys.* 176 (1993) 233.
- [22] W.P. de Boeij, M.S. Pshenichnikov, K. Duppen and D.A. Wiersma, *Chem. Phys. Letters* 224 (1994) 243.
- [23] M.S. Pshenichnikov, K. Duppen and D.A. Wiersma, *Phys. Rev. Letters* 74 (1995) 674.
- [24] P. Vöhringer, D.C. Arnett, R.A. Westervelt, M.J. Feldstein and N.F. Scherer, *J. Chem. Phys.* 102 (1995) 4027.
- [25] T. Joo, Y. Jia and G.R. Fleming, *J. Chem. Phys.* 102 (1995) 4063.
- [26] P. Vöhringer, D.C. Arnett, T.-S. Yang and N.F. Scherer, *Chem. Phys. Letters* 237 (1995) 387.
- [27] W.P. de Boeij, M.S. Pshenichnikov and D.A. Wiersma, *Chem. Phys. Letters* 238 (1995) 1.
- [28] S. Mukamel, *Principles of nonlinear optical spectroscopy* (Oxford University Press, New York, 1995).
- [29] S. De Silvestri, A.M. Weiner, J.G. Fujimoto and E.P. Ippen, *Chem Phys. Letters* 112 (1984) 195.
- [30] A.M. Weiner, S. De Silvestri and E.P. Ippen, *J. Opt. Soc. Am. B2* (1985) 654.
- [31] D.A. Wiersma, invited paper: Time-resolved femtosecond photon echo as probe of solvent motion, VII-th Time-resolved Vibrational Spectroscopy Meeting (Santa Fé, New Mexico, 11–16 June, 1995).
- [32] R.W. Schoenlein, D.M. Mittleman, J.J. Shiang, A.P. Alivisatos and C.V. Shank, *Phys. Rev. Letters* 70 (1993) 1014.
- [33] M.S. Pshenichnikov, W.P. de Boeij and D.A. Wiersma, unpublished results.
- [34] W.P. de Boeij, M.S. Pshenichnikov and D.A. Wiersma, *Chem. Phys. Letters* 247 (1995) 264.
- [35] W.P. de Boeij, M.S. Pshenichnikov and D.A. Wiersma, *J. Chem. Phys.* (1995) submitted.